

Two-dimensional electron gas as a flux detector for a type-II superconducting film

S. J. Bending,* K. von Klitzing, and K. Ploog

Max-Planck-Institut für Festkörperforschung, Heisenbergstrasse 1, D-7000 Stuttgart 80, West Germany

(Received 15 June 1990)

Thin type-II superconducting films have been prepared on top of the two-dimensional electron gas (2DEG) in a GaAs/Al_{1-x}Ga_xAs heterostructure. The type-II gate and the 2DEG are so close to one another that the magnetic field distribution at the superconductor, consisting of a lattice of flux vortices, is projected intact onto the electronic system below. We show that the 2DEG acts as a very sensitive flux detector for the superconducting film. Both the Hall voltage (V_H) and the magnetoconductance (σ_{xx}) reflect the irreversible motion of flux in the gate in complementary ways. In particular, σ_{xx} is a probe of magnetic-field inhomogeneities on a scale of the inelastic scattering length in the 2DEG. A method of measuring the spatial dependence of the magnetic field at a flux vortex is proposed that exploits this property.

I. INTRODUCTION

Semiconductor Hall probes have been used for a great many years as magnetic flux detectors in reasonably uniform magnetic fields. However, in cases where the field distribution is strongly spatially inhomogeneous, semiconductor probes have the potential to yield much more information than simply the spatially averaged value of the magnetic field. An obvious example where this would be valuable is in a type-II superconducting film above the lower critical field H_{c1} when the magnetic field enters the superconductor as flux vortices containing a single flux quantum ($h/2e$). In this case the semiconductor probe could yield details about the microscopic flux distribution present if it was in such intimate contact with the superconducting film that the inhomogeneous field distribution was projected intact down onto it.

An estimate of the maximum allowable separation between the two-dimensional electron gas (2DEG) and superconducting film can be obtained if one knows the spatially dependent magnetic field at the surface of the superconductor. The distribution in a plane a perpendicular distance z away can be calculated by performing a Fourier transformation of Maxwell's equations.¹ Assuming the field is present as an ordered lattice of flux tubes, one finds

$$B_z(\mathbf{r}, z) = \sum_{\mathbf{q}} \tilde{B}_z(\mathbf{q}, 0) \exp(-|\mathbf{q}|z) \exp(i\mathbf{q} \cdot \mathbf{r}), \quad (1)$$

where $\tilde{B}_z(\mathbf{q}, 0)$ is the Fourier transform of the field distribution at the sample surface, and \mathbf{q} must be summed over all the fluxoid lattice wave vectors. Clearly, the Fourier components of the inhomogeneity become exponentially damped as z increases. At a given field the condition that the lowest Fourier component of the lattice still remains somewhat intact is $|\mathbf{q}_0|z < 1$. In a mean field of 100 G, this will be satisfied when $z < 100$ nm. Such a stringent condition can only be fulfilled by integrating the superconductor and detector into one single hybrid structure, and by confining the z extent of the charge carriers in the

semiconductor probe as far as possible to a single plane. Two obvious device candidates which meet these requirements spring to mind. One could fabricate the gate of a silicon metal-oxide-semiconductor field-effect transistor (MOSFET) out of a type-II superconducting material. Some measurements on structures of this nature have been reported elsewhere.² The second possibility, and the one studied here, is to deposit a type-II superconducting film on top of a GaAs/Al_{1-x}Ga_xAs heterostructure two-dimensional electron gas. In both cases the charge carriers in the detector are confined to a layer less than 10 nm thick, and a reduction of the gate-channel separation below 100 nm is a relatively simple task.

Measurements of two distinct parameters at the 2DEG, the Hall voltage (V_H), and the magnetoconductance ($\Delta\sigma = \Delta\sigma_{xx} = -\Delta\rho_{xx}/\rho_{xx}^2$) will be presented here as a function of applied magnetic field. Both reflect all the irreversible effects associated with flux motion in type-II superconducting films, i.e., delayed flux entry and exit, flux pinning, and flux jumps. In the low-applied-field regime, the distribution at the 2DEG takes the form of spatially resolved flux vortices. In this limit the Hall voltage is linearly proportional to the *net* flux threading the detector (difference of "up" and "down" vortices), while $\Delta\sigma_{xx}$ is some function of the *total* number of vortices present (both up and down). Clearly, the two measurements are complementary and, given the existence of a quantitative theory for $\Delta\sigma_{xx}$, enable the fraction of up or down fluxoids present to be precisely determined.

In addition, if the detector is chosen so that its low-temperature magnetoresistance is a consequence of the suppression of weak localization effects,³ then the characteristic transport length scales in the 2DEG can be varied in order to probe the scale of the magnetic-field inhomogeneity. In quasiclassical terms weak localization is a quantum correction to the Drude conductivity arising due to the constructive backscattering of time-reversed classical diffusive paths. Only paths which maintain quantum phase coherence are important, and so the characteristic length scale for this process is the inelastic

scattering length l_i ($l_i = \sqrt{D\tau_i}$, where D is the electron diffusion constant and τ_i is the inelastic scattering time). The time-reversal symmetry is broken by the application of a magnetic field, leading to the negative magnetoresistance characteristic of such structures. Thus $\Delta\sigma_{xx}$ probes the magnetic field inhomogeneity on a scale of l_i .

II. SAMPLE STRUCTURE AND EXPERIMENTAL DETAILS

The data presented here represent samples with three different superconducting gate materials, 200 nm lead (Pb), 400 nm of a lead/indium [Pb(1 at. % In)] alloy, and 200 nm of niobium nitride (NbN). These were chosen as being materials whose characteristic superconducting length scales span a broad range. The crossover from type-I (intermediate) to type-II (mixed) superconducting behavior occurs in bulk materials when the ratio of the magnetic-field penetration depth (λ_L) and the superconducting coherence length (ξ) exceeds $1/\sqrt{2}$. Bulk Pb is known to be type I ($\lambda_L/\xi \sim 0.5$), but in sufficiently thin-film form becomes type II for two reasons. First, the elastic mean free path is reduced in the film by surface and grain-boundary scattering, leading to an increase in λ_L . Second, Tinkham has shown⁴ that demagnetization effects in thin films make large type-I-like domains energetically unfavorable. Indeed, Dolan⁵ has performed decoration experiments on Pb films deposited under almost identical conditions to those here and finds that the flux is present as fluxoids of single (mixed state) or multiple flux quanta (transitional state). The Pb film which has been alloyed with 1% of In lies well inside the type-II regime on account of an increase in λ_L due to random alloy scattering. Both the Pb and Pb (1 at. % In) films were thermally evaporated onto the GaAs chips at ambient temperatures. The third material, NbN, was dc-magnetron sputtered from a Nb target onto a water-cooled sample in a mixture of nitrogen and argon gases. Sputtered NbN is a granular material and in our case is probably composed of columnar grains about 20 nm in diameter.^{6,7} Such films are very strongly type II ($\lambda_L/\xi > 40$). A disadvantage of sputter deposition as opposed to evaporation is that it causes quite large changes in the mobility of the underlying 2DEG due to damage by high-energy ion bombardment. It was found, however, that this damage could be almost completely removed by tempering the sample for an hour at quite low temperatures ($\sim 260^\circ\text{C}$).

During the course of this work, several different GaAs 2DEG's were used. The data presented here represent devices fabricated in only two of these. The NbN-gated samples were formed from pieces of a fairly standard wafer grown to achieve high low-temperature electron mobilities ($\mu = 325\,000\text{ cm}^2\text{V}^{-1}\text{s}^{-1}$, $n_{2D} = 3.03 \times 10^{11}\text{ cm}^{-2}$). While effects seen in V_H were very similar to those observed in low-mobility samples, the magnetoresistance was qualitatively different. Indeed, a positive magnetoresistance was observed in the NbN-gated samples at low fields which could not be attributed to weak localization effects. Although this positive magnetoresistance also showed hysteretic effects reflecting flux motion

in the NbN film, it will not be presented here for want of a quantitative theory to interpret it.

The Pb and Pb (1 at. % In) films were both prepared on pieces from the same heterostructure whose quality had been deliberately degraded to ensure the dominance of weak localization effects in the magnetoresistance. This was achieved by using a very short (30-nm) GaAs buffer layer between the wafer substrate and the 2DEG. This would normally be at least an order of magnitude thicker to prevent the possibility of unwanted impurities riding at the growth surface reaching the active region of the device near the GaAs/ $\text{Al}_{1-x}\text{Ga}_x\text{As}$ interface. At low temperatures it was found that the presence of the evaporated gates led to the depletion of the 2DEG beneath them. This was overcome by a short photoexcitation with a red light-emitting diode which established a stable electron density by virtue of the persistent photoconductivity effect.⁸ In the measurements presented here, the carrier mobility and two-dimensional density for the Pb [Pb(1 at. % In) sample at 4.2 K were $17\,900\text{ cm}^2\text{V}^{-1}\text{s}^{-1}$ ($17\,900\text{ cm}^2\text{V}^{-1}\text{s}^{-1}$) and $1.98 \times 10^{11}\text{ cm}^{-2}$ ($1.98 \times 10^{11}\text{ cm}^{-2}$).

In practice, chips 5 mm square were cut from the GaAs wafers, and Hall bars, 1 mm long and $100\ \mu\text{m}$ wide, with large current contacts at the ends and three pairs of voltage contacts along the sides were etched into them (see the schematic diagram in the inset of Fig. 1). After gate deposition and bonding, the chips were mounted onto a temperature-controllable sample holder which was evacuated and slid inside a solenoid made of high-purity copper wire. The entire insert was then immersed in a bath of liquid helium and the sample temperature stabilized to better than $\pm 5\text{ mK}$ with a commercial controller. A calibrated carbon-glass resistor was used to read off the temperature in zero field and a capacitance thermometer to control temperature during field sweeps. The magnetic field at the sample was calculated taking into account the finite wire thickness and solenoid length, and was cross-checked with a commercial Hall-probe gaussmeter.

All measurements were performed at 15 Hz with an rms ac current of 300 nA flowing between current con-

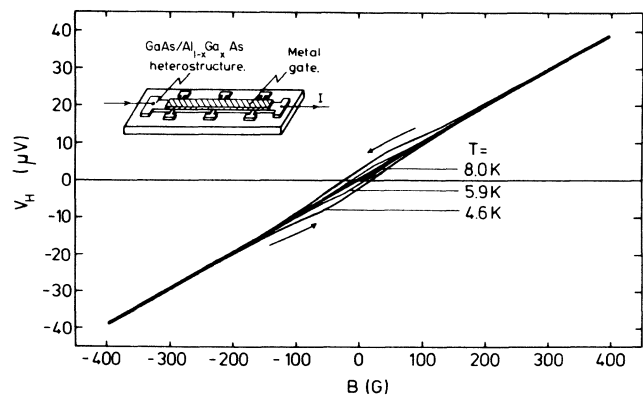


FIG. 1. Hall voltage at 2DEG plotted against applied magnetic field for a Pb-gated sample cycled at three different temperatures. Inset shows sketch of a typical device.

tacts in the 2DEG. The Hall voltage was measured directly at the sample with a lock-in amplifier and changes in the longitudinal resistivity ρ_{xx} detected with a sensitive ac resistance bridge.

III. MEASUREMENTS ON THE HALL VOLTAGE

Figure 1 shows a plot of the Hall voltage measured at the 2DEG on a Pb-gated device as a function of the applied magnetic field at three different temperatures. In each case the sample was cooled below T_c (7.2 K) at zero field, swept up to positive fields, and subsequently down and up cyclically. Note that when the temperature is above T_c one observes the classical Hall voltage linear in B . However, below T_c the curves trace out a hysteric loop, reflecting the irreversible motion of flux in the lead gate. The data have been deliberately presented on a rather coarse scale in Fig. 1 to indicate the range of fields over which the hysteresis persists. At 4.6 K the up and down sweeps are quite easily distinguishable out to ± 200 G.

Figures 2–4 show V_H hysteresis loops on a more sensitive field scale for the three different gate materials, Pb, Pb (1 at. % In), and NbN, respectively. As before, the measurements begin by cooling through T_c at $B=0$ G followed by sweeping the field in the direction of the arrows shown at a rate of about 1 G/s. Note that the hysteresis loop appears to have been established after just a single cycle and does not change appreciably upon further cycling. All three gate materials show strikingly similar behavior despite having substantially different superconducting properties. Nevertheless, a more detailed examination of the data does reveal small differences which one might anticipate on the basis of the microstructure of the films. When the Hall voltage is zero, the superconducting film must contain equal numbers of up and down flux vortices. Fluxoids whose direction opposes that of the applied field represent flux metastably trapped in the film; hence the field at the zeros of V_H is a measure of the strength of flux pinning. As we follow the series Pb, Pb (1 at. % In), NbN, one observes that the width of the hysteresis loops along $V_H=0$ does progres-

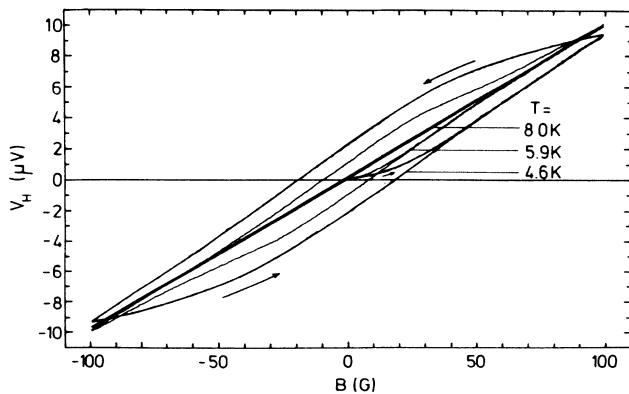


FIG. 2. Hall voltage at 2DEG plotted against applied magnetic field for a Pb-gated sample cycled at three different temperatures.

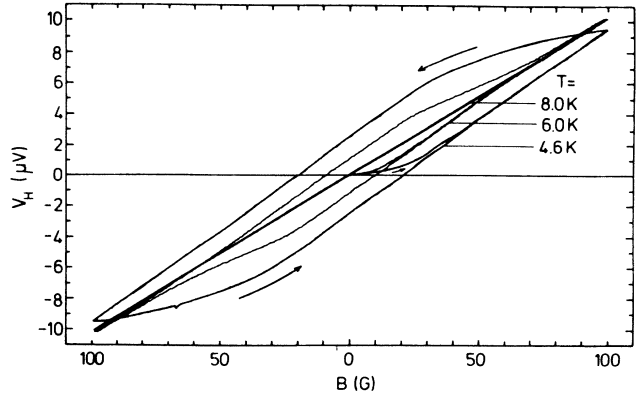


FIG. 3. Hall voltage at 2DEG plotted against applied magnetic field for a Pb (1 at. % In)-gated sample cycled at three different temperatures.

sively increase, indicating stronger pinning. This is broadly what one would anticipate on the basis of the reduction in grain size in the films along the series leading to an increase in total length of the grain boundaries and stronger pinning. A second source of pinning, sometimes called *edge pinning*, arises due to the existence of a Gibbs-free-energy barrier to flux entry (or exit) at the edge of the film. This was first calculated by Clem, Huebener, and Gallus,⁹ who give approximate results for the field at which flux enters at the edge of a type-II superconductor in the limit that t , the thickness of the superconductor, is very much greater than λ_L . These authors find that the edge barriers to flux entry are overcome above a field $H_{en}(0)$:

$$H_{en}(0) = H_{c1} \left[1 + \left(\frac{2\sqrt{w\lambda_L}}{t \ln(\lambda_L/\xi)} \right) \right], \quad (2)$$

where H_{c1} is the lower critical field for the type-II superconductor in the absence of edge pinning, and w is the width of the film. This limit is, however, not really appropriate for our films, which are not very much thicker than λ_L . Nevertheless, one would qualitatively expect progressively higher barriers to flux entry at the edges as

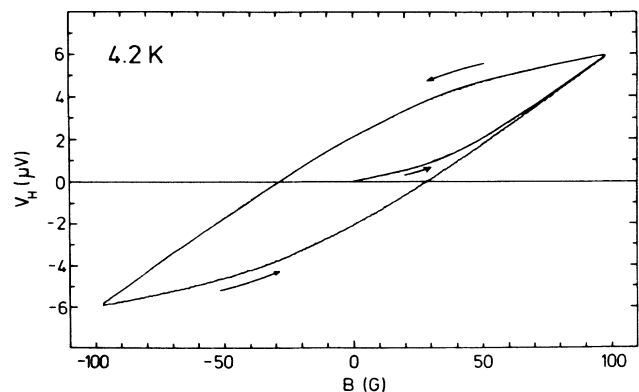


FIG. 4. Hall voltage at 2DEG plotted against applied magnetic field for a NbN-gated sample cycled at 4.2 K.

λ_L increases. By the same token flux will be metastably trapped inside the film for fields below H_{c1} , and the strength of this effect will also depend on λ_L . Edge pinning would then also be expected to increase as one descends the series of materials due to the associated increases in λ_L with the exception of the Pb (1 at. % In) films, which are twice as thick as the others.

Figure 5 shows a single field cycle for the NbN-gated sample at 1.5 K. The structure was cooled below T_c (12.5 K) at $B=0$ G; the field was then swept up to about 350 G, halted, and swept down again. The sweep rate used of 4 G/s was somewhat faster than used elsewhere. The striking feature of Fig. 5 is the sudden drop in Hall voltage on the downward sweep near $B=65$ G. This represents the sudden exit of a large number of vortices from the film. The flux jump was always present upon further cycling, although its position tended to vary a little. Moreover, the same jump could be observed at different pairs of voltage contacts, indicating that it is a macroscopic effect, and we estimate that between 10^4 and 10^5 individual vortices are involved.

Flux jumps are an established phenomenon in type-II superconductors and arise due to the rigidity of the vortex lattice formed in a magnetic field. As a consequence, a few strong pinning centers can anchor a "raft" comprised of a very large number of fluxoids. However, when the external conditions (e.g., B , T , or J) are altered to the point where the pinning force at one of the centers can just be overcome, local vortex displacements can take place. This motion generates heat due to dissipative processes, e.g., eddy current damping in the normal vortex core. Generated heat leads in turn to a further weakening of the pinning force and in the right circumstances can cause an avalanche breakdown of pinning and macroscopic flux flow. The rate of heat dissipation (and, e.g., the field sweeping rate) is clearly an important parameter since there is a competition with the thermal conductance of heat away from the generation center.

IV. MEASUREMENT OF THE MAGNETOCONDUCTANCE

Figures 6 and 7 show magnetoconductance data for the same Pb- and Pb (1 at. % In)-gated samples shown in

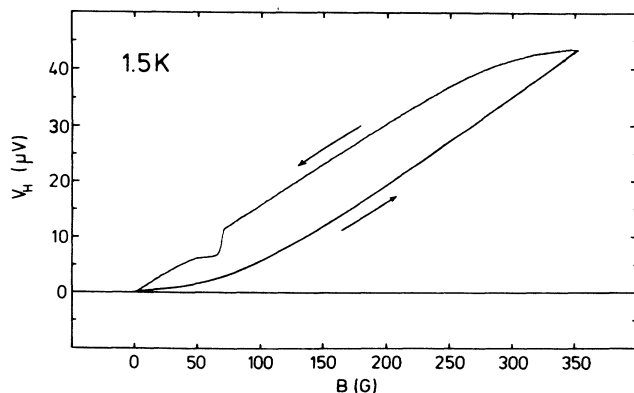


FIG. 5. Hall voltage at 2DEG for a NbN-gated sample at 1.5 K showing a flux jump on the downward sweep of the cycle.

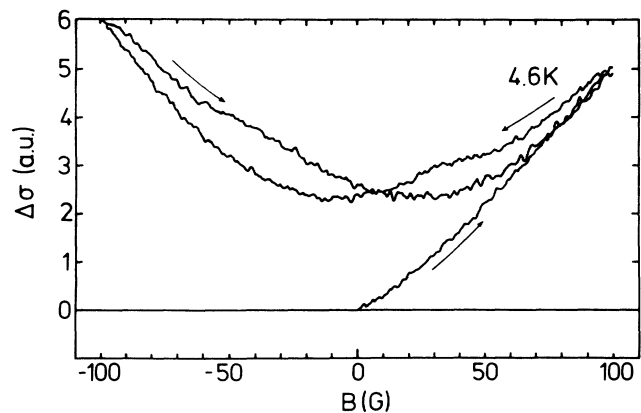


FIG. 6. Magnetoconductance at 2DEG plotted against applied magnetic field for a Pb-gated sample cycled at 4.6 K.

Figs. 2 and 3, respectively. In each case the sample was cooled below T_c at $B=0$ G and the field then swept in the direction of the arrows at a rate of 1 G/s. Note the dramatic differences between Figs. 6 and 7 despite the very strong similarities of plots of the Hall voltage for the identical field cycles.

Figure 6 contains data for the Pb-gated sample at 4.6 K. As the field is initially increased from 0 to 100 G, the conductance increases strongly (negative magnetoresistance) due to the suppression of weak localization corrections in the 2DEG. Upon reversal of the sweep direction, the magnetoconductance shows a weak shoulder due to delayed flux exit from the Pb film. At about 50 G a second-quite pronounced shoulder develops, indicating that a second flux pinning mechanism is coming into operation. We tentatively identify edge pinning as being the mechanism responsible for this second shoulder, while the delayed flux exit upon reversal of the sweep direction at 100 G is more likely to be due to microscopic pinning centers within the film. The conductance eventually reaches a minimum near $B = -15$ G with a value somewhat in excess of that at the cycle origin due to the continued presence of trapped flux in the superconducting gate. If we assume that the magnetoconductance is a function of the total number of up and down vortices

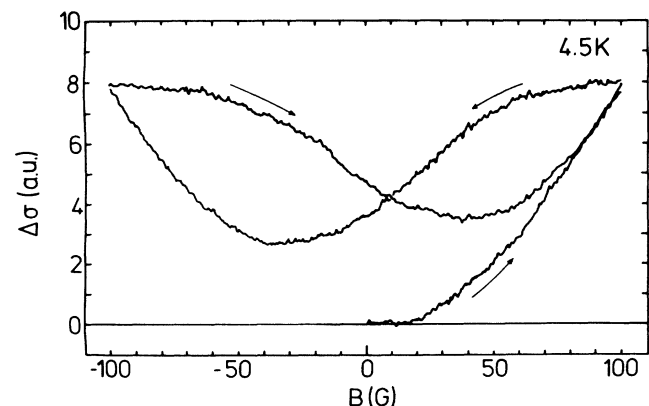


FIG. 7. Magnetoconductance at 2DEG plotted against applied magnetic field for a Pb (1 at. % In)-gated sample at 4.5 K.

$[\Delta\sigma = f(N_{\uparrow} + N_{\downarrow})]$, then the conductance minima represent the fields at which the total number of vortices is minimized. After the second reversal the same features are present, but reflected about the y axis, yielding a bow-shaped cyclic structure. Once again the structure was well established after a single cycle and changed very little upon further cycling. Residual asymmetry in the bow-shaped curve almost certainly arises from a small percentage of the Hall voltage being mixed into the signal as a result of very weak spatial inhomogeneities in the 2DEG.

Figure 7 presents data from the Pd (1 at. % In)-gated sample at 4.5 K. This shows a number of important differences from the Pb data. When the magnetic field is first increased, the magnetoconductance change is strongly suppressed up to about 15 G. Similarly, upon reversal of the sweep direction, $\Delta\sigma$ shows broad shoulders of weak magnetic-field dependence. Both effects point to strongly delayed flux entry and flux exit due to strong microscopic pinning centers within the superconducting film. As a consequence, the bow-shaped structure is much deeper in relation to the separation between the magnetoconductance minima at about ± 40 G and the origin of the cycle. Furthermore, there is no evidence of a second shoulder in the curves away from the field-reversal positions consistent with the weakening of edge pinning in these thicker films, though this may simply have been masked by the much stronger "bulk" pinning.

V. DISCUSSION

Clearly, both V_H and σ_{xx} reflect the irreversible motion of flux in the type-II superconducting gates. V_H is a measure of the net flux threading the hybrid device and is proportional to the difference in the number of up and down vortices present. As it is insensitive to vortex overlap and smearing due to the finite separation of the gate and 2DEG, measurements of the Hall voltage in the hybrid devices described here are really an example of the conventional use of semiconductor Hall probes as sensors of the mean magnetic field. In this mode the detector is not sensitive to field inhomogeneities and internal flux structures, with the consequence that hysteresis loops for gate materials with considerably different superconducting length scales appear very similar. However, upon detailed examination weak effects due to changes in the penetration depth and pinning force are discernible in the width of the hysteresis loops. Because of the relatively small size of the superconducting films one can measure in this way, fairly small-scale dynamic effects, e.g., flux jumps, are very clearly reflected in V_H .

The magnetoconductivity due to an isolated vortex does not depend on whether it is oriented upwards or downwards. Thus the low-field magnetoconductivity is a function of the total number of fluxoids present, both up and down. Overlap between vortices causes the distinction between up and down vortices to be lost, and the magnetoconductance weakens due to partial cancellation of the field distributions. For this reason the measurement is strongly sensitive to inhomogeneities of the flux distribution. Furthermore, the weak localization correction due to a single magnetic flux vortex is qualitatively

different from the equivalent homogeneous field result, and depends on the relative sizes of the radius of the flux tube (r_0) and the inelastic scattering length (l_i) in the 2DEG. Rammer and Shelankov¹ have calculated the magnetoconductance for this problem and give closed results in certain limiting cases. If $r_0 \gg l_i$, then

$$\sigma_L(B, T) - \sigma_L(0, T) \approx \frac{1}{24} \frac{e^2}{2\pi^2\hbar} \frac{B_0}{B_i} \left[\frac{|B|}{B_i} \right], \quad (3)$$

where the field within the flux tube is assumed constant and equal to B_0 , and B_i is the characteristic "inelastic field" ($B_i = \Phi_0/4\pi l_i^2$). On the other hand, if $r_0 \ll l_i$ and the mutual separation of the tubes is greater than l_i (narrow isolated tubes), then

$$\sigma_L(B, T) - \sigma_L(0, T) \approx \frac{e^2}{2\pi^2\hbar} \frac{1}{N \ln(B_0/NB_i)} \left[\frac{|B|}{B_i} \right], \quad (4)$$

where the fluxoid has been assumed to contain N flux quanta. In all cases the magnetoconductance is linear in $|B|$, in sharp contrast to the B^2 result for homogeneous fields in the low-field limit,³ and the prefactor is a measure of B_0 . Rammer and Shelankov have, however, made the simplifying approximation that a flux tube consists of a cylinder of uniform magnetic field. For our case of superconducting vortices, this is clearly not very realistic, and a full calculation would be needed taking into account the spatial dependence of the magnetic field in a vortex core in order to obtain quantitative agreement between experiment and theory. Nevertheless, assuming that $B_0 \approx \Phi_0/\pi\lambda_L^2$ for a strongly type-II superconductor, we see that the prefactor of Eq. (3) or (4) yields a direct measure of the magnetic-field penetration depth in the film.

Consequently, the striking differences between Figs. 6 and 7 arise not only because of different pinning effects in the superconducting films, but also due to differences in the penetration depth λ_L and its relation to the inelastic scattering length in the 2DEG detector. A more detailed study of this second effect is published elsewhere.¹⁰ In principle, the measurement of the magnetoconductance for a range of different inelastic scattering lengths allows one to infer the spatially dependent magnetic field around the vortex core, something which has never been measured before. This could be realized by applying a bias voltage between the superconducting gate and the 2DEG in order to vary the 2D electron density (and mobility), and monitoring the magnetoconductance as l_i is tuned through a broad range of values.

VI. CONCLUSIONS

In conclusion, we have studied the use of a two-dimensional electron gas in a GaAs/Al_{1-x}Ga_xAs heterostructure as a flux detector for type-II superconducting films deposited on top of it. Both the Hall voltage and magnetoconductance measured at the 2DEG reflect the irreversible motion of magnetic flux in the superconductor, the former being sensitive to the net flux threading the detector and the latter to the total number of vortices present. The Hall voltage is insensitive to inhomogeneity

genities in the field distribution, and in this mode the detector operates in essentially the same way as conventional semiconductor Hall probes. However, because of the very small size of the measured superconducting samples, fairly small-scale dynamic effects, e.g., flux jumps, can be easily detected. The magnetoconductance is, on the other hand, strongly sensitive to inhomogeneities in the field distribution and yields a wealth of information about flux structures, their characteristic length scales, and the various pinning mechanisms in type-II films. In particular, if one were to vary the inelastic scattering length in the 2DEG by applying a "gate voltage" to the structure, one could infer the spatial dependence of the magnetic-field distribution at a vortex.

Future work will focus on developing the techniques described here in detector structures which are so small that they contain only one or two flux vortices. This

should not only make the presented phenomena much easier to observe, but will also facilitate their theoretical treatment and understanding. It is also planned to study flux flow in high- T_c superconducting films in specially designed composite structures.

ACKNOWLEDGMENTS

The authors thank M. Hauser for expert help with the sample preparation and I. Jungbauer and F. Scharfner for processing and bonding. We are indebted to H.-J. Hedbavny and H. Rogalla for depositing the NbN gates. We would like to acknowledge valuable discussions with A. L. Shelankov, T. M. Klapwijk, G. H. Kruithof, and J. Chalker. Part of this work was sponsored by the Bundesministerium für Forschung und Technologie of the Federal Republic of Germany.

*Present address: University of Bath, School of Physics, Claverton Down, Bath BA2 7AY, England.

¹J. Rammer and A. L. Shelankov, *Phys. Rev. B* **36**, 3135 (1987).

²G. H. Kruithof and T. M. Klapwijk, in *Proceedings of the 19th International Conference of The Physics of Semiconductors*, Warsaw, 1988, edited by W. Zawadzki (Wroclawska Drukarnia Naukowa, Warsaw, 1988).

³B. L. Altshuler, D. Khmel'nitzkii, A. I. Larkin, and P. A. Lee, *Phys. Rev. B* **22**, 5142 (1980).

⁴M. Tinkham, *Phys. Rev.* **129**, 2413 (1963).

⁵G. J. Dolan, *J. Low Temp. Phys.* **15**, 111 (1974).

⁶H. L. Ho, R. T. Kampwirth, K. E. Gray, D. W. Capone II, L. S. Chumbley, and M. Meshii, *Ultramicroscopy* **22**, 297 (1987).

⁷S. Thakoor, J. L. Lamb, A. P. Thakoor, and S. K. Khanna, *J. Appl. Phys.* **58**, 4643 (1985).

⁸D. V. Lang, R. A. Logan, and M. Jaros, *Phys. Rev. B* **19**, 1015 (1979).

⁹J. E. Clem, R. P. Huebner, and D. E. Gallus, *J. Low Temp. Phys.* **12**, 449 (1973).

¹⁰S. J. Bending, K. von Klitzing, and K. Ploog, *Phys. Rev. Lett.* **65**, 1060 (1990).